CHARACTERISTICS OF HEAT TRANSFER AND PRESSURE DROP IN A CHEVRON-TYPE PLATE HEAT EXCHANGER WITH AL_2O_3/WATER NANOFLUIDS

Murat UNVERDI**, Yasar ISLAMOGLU
Department of Mechanical Engineering, Sakarya University, Sakarya, Turkey
E-mail: muratunverdi@gmail.com

In this study, heat transfer and pressure drop characteristics have been experimentally investigated by using Al_2O_3/water nanofluids in the chevron-type plate heat exchanger. The purpose of the experiments was to determine the heat transfer coefficient and pressure drop for different flow rates of 90, 120, 150, 180, 240 and 300 kg/h and different volume concentrations of 0.25%, 0.5%, 0.75% and 1% of the nanofluids. The Nusselt number of the nanofluids increased with the increasing volume concentration and flow rate at constant hot water flow rate and constant inlet temperatures. The increase in the Nu number is 42.4% when compared to distilled water at the maximum volume concentration and Reynold number (600≤Re≤1900) in the nanofluids-plate heat exchanger. It has been concluded that nanofluids enhanced the heat transfer significantly and pressure drops at the maximum volume concentration and the Reynold number increased by between 6.4% and 8.4% compared to distilled water.

Keywords: *Nanofluids, Plate heat exchanger, Heat transfer, Pressure drop*

1. Introduction

In the studies conducted in recent years, miniaturization of the large heat transfer equipment and high-performance heat transfer fluids have been needed to fulfill the industrial requirements. Current technology has reached its limits in terms of the miniaturization of the equipment that will ensure the heat transfer needed by the industry. The idea behind the improvement of the nanofluids is to increase the heat transfer coefficient by using these fluids as working fluids in the equipment that will ensure heat transfer and also to decrease the sizes of the large equipment that will ensure heat transfer. For this reason, it is required to improve the high-performance heat transfer fluids. Flow and heat transfer characteristics of these fluids are changed by adding suspended solid particles into the working fluids (water, oil, ethylene glycol, etc.). High-performance heat transfer fluids are obtained by changing the thermo-physical characteristics of the working fluid (thermal conductivity, specific heat, density, and viscosity) and also through the addition of metallic and non-metallic particles with the sizes structurally varying between 1 and 100 nanometers, which are suspended in the working fluid **[1-6]**. In the literature, experimental studies have been extensively carried out to enhance the heat transfer by using nanofluids in the channels with various flow geometries. Heris et al.'s **[7]** investigated nanofluids containing CuO and Al_2O_3 oxide nanoparticles in water as a base fluid in different concentrations produced and the laminar flow convective heat transfer through a circular tube with the constant wall temperature boundary condition. The experimental results indicate that the heat transfer coefficient improves with increasing nanoparticles concentrations for both nanofluids systems. The heat transfer enhancement for 2.5% concentration of each nanofluids is higher than that of 3.0% and therefore the optimum concentration of Al_2O_3 and CuO nanoparticles are between 2.5% and 3.0%. The experimental study by Anoop et al.'s **[8]** on the convective heat transfer characteristics in the developing region of the tube flow with the constant heat flux was carried out with alumina–water nanofluids. Two particle sizes were used in the study, one with the average particle size of 45 nm and another one with 150 nm. It was observed that both nanofluids showed higher heat transfer characteristics compared to the base fluid, while the nanofluid with 45 nm particles showed a higher heat transfer coefficient in comparison to the 150 nm particles. It was further observed that the nanofluid with 45 nm particles shows higher heat transfer coefficient than that with 150 nm particles. For 45 nm particle based nanofluid (4 wt%) the enhancement in heat transfer coefficient was around

25% whereas for the 150 nm particle based nanofluids it was found to be around 11%. Xu and Xu **[9]** investigated the flow boiling heat transfer in a single microchannel with pure water and nanofluid (weight concentration of 0.2%, 40 nm) as the working fluids. The experimental results show the enhancement of the heat transfer with nanofluid compared to pure water. The heat transfer coefficient for nanofluid is about 17% higher than that for pure water. Edalati et al.'s **[10]** investigated the heat transfer of an equilateral triangular duct by employing the CuO/water nanofluid in a laminar flow and under the constant heat flux condition. The results of their study show that the experimental heat transfer coefficient of the CuO/water nanofluid is more than that of distilled water. Moreover, the experimental heat transfer coefficient of the CuO/water nanofluid is greater than the theoretical one. At a 0.8% concentration of CuO/water nanofluid, the convective heat transfer coefficient ratio changes from 1.36 to 1.41. Hojjat et al.'s **[11]** investigated the forced convection heat transfer under the laminar flow conditions experimentally for three types of non-Newtonian nanofluids (γ-Al_2O_3, TiO_2, and CuO) in a circular tube with the constant wall temperature. The results of their study show that the presence of nanoparticles increases the convective heat transfer of the nano-dispersions in comparison with the base fluid. The average increases of the Nusselt number for nanofluids with 0.1, 0.2, 0.5, 1.0, and 1.5 volume percents of nanoparticles are about 8, 10, 12, 17, and 19% for γ -Al2O3 nanofluids, about 8, 11, 14, 17, and 21% for CuO nanofluids and about 6, 9, 11, 15, and 16% for TiO_2 nanofluids. In the study conducted by Sommers and Yerkes **[12]**, dilute suspensions of 10 nm aluminum oxide nanoparticles in propanol (0.5, 1, and 3 wt %) were investigated. They found that for the 1 wt % concentration, a small but significant enhancement (~15-20%) in the heat transfer coefficient was recorded for $1800 < Re < 2800$, which is attributed to an earlier transition to the turbulent flow. In the case of high particle loading (3 wt %), the thermal performance was observed to deteriorate with respect to the baseline case. Tiwari et al.'s **[13]** have undertaken experimental investigations to explore the heat transfer and pressure drop characteristics in a chevron-type corrugated plate heat exchanger using CeO_2/water nanofluids as the coolant. They found out that the heat transfer coefficient of the nanofluids increases (~39%) with an increase in the volume flow rate of the hot water and nanofluids and also with a decrease in the nanofluids temperature. In the study conducted by Huang et al.'s **[14]**, heat transfer and pressure drop characteristics of Al_2O_3/water and MWCNT/water nanofluids flowing in a chevron-type plate heat exchanger were experimentally investigated and compared with those of water. Results showed that little heat transfer enhancement was observed. The results of the study showed that heat transfer seemed to be improved by using nanofluids at the constant Reynolds number. However, little heat transfer enhancement was observed based on a constant flow velocity. In this study, the increase in the heat transfer was researched by using nanofluids instead of distilled water in the gasket plate heat exchanger, a corrugated surfaced plate, which is one of the various passive techniques used for the enhancement of the heat transfer. The difference of this study from the previous nanofluids corrugated surface plate heat exchangers in the literature is its applicability to the systems operating below room temperature and in the cooling of the systems exposed to the low heat load at the operating temperature (not exceeding 50^oC), in which high heat transfer is desired at low temperature differences (electronic devices, in growing vegetables in greenhouses with geothermal fluid, etc.), in addition to the absence of an experimental study for the geometric dimensions, selected nanoparticle size, and concentrations for the plate heat exchanger.

2. Experimental investigation

2.1. Preparation of the nanofluids

Nanopowders were added into the distilled water at the desired volumetric proportion to prepare the nanofluid suspension. In this study, alpha Al_2O_3 nanopowders with the average diameter of 40 nm and the purity of 99.9% were used. Furthermore, no dispersant and stabilizer were used not to change the fluid characteristics. In this study, four different Al_2O_3/water nanofluids concentrations were prepared. The amount of nanoparticles required to prepare 1 l of the nanofluid was calculated as in Ref. **[15]**.

$$m_{np} = \emptyset_{np}\text{x1x}10^{-3}\rho_{np} \quad (1)$$

Here, $\emptyset_{np}$ refers to the volume concentration of the mixture and ρ_{np} indicates the density of the nanoparticles, while m_{np} symbolizes the mass of the nanoparticles which must be added to the mixture. Nanoparticle density was $3700\,kg/m^3$ in the calculations and taken from Ref. **[16]**. Nanopowders were added into the distilled water at the calculated amount and dispersed homogenously and prevented from agglomeration by using the ultrasonic bath (model Cneumaw) and mechanic mixer for 1 hour. No sedimentation was observed in the prepared mixtures for 6 hours on average **[17- 19].**

2.2. Determination of the thermophysical characteristics of the nanofluids

In order to obtain reliable experimental results, the expressions suggested in the literature for the calculation of the thermophysical characteristics of the nanofluids were used. These characteristics consist of the pre-derived density, viscosity, specific heat and thermal conductivity Eq.s. Thermophysical characteristics of the nanofluids were calculated with classic approach formulas using the average temperature values with the assumption that nanoparticles dispersed homogeneously in the distilled water. The below-stated Eq.s were used in this study.

Density of nanofluids,

$$\rho_{nf} = \left(1 - \emptyset_{np}\right)\rho_s + \emptyset_{np}\rho_{np} \quad (2)$$

Pak and Cho and Ho et al.'s showed the validity of the Eq. (2) and the density of Al_2O_3-water nanofluids at the room temperature with their experiments. They concluded with the experimental results that the nanofluids were in excellent concordance with Eq. (2) used for the estimation of its density **[20-23]**.

Dynamics viscosity of nanofluids,

$$\mu_{nf} = \left(1 + 2.5\emptyset_{np}\right)\mu_s \quad (3)$$

Eq. (3) is the Einstein Eq. and can be accepted for less spherical particles at 2% volume concentration **[23-25]**.

Specific heat of nanofluids,

$$c_{p,nf} = \left(\left(1 - \emptyset_{np}\right)\rho_s c_{p,s} + \emptyset_{np}\rho_{np}c_{p,np}\right)/\rho_{nf} \quad (4)$$

Zhou and Ni showed the validity of Eq. (4) and the specific heat of the Al_2O_3-water nanofluids at the room temperature with their experiments. They concluded that the nanofluids were in a very good concordance with Eq. (4) used for the estimation of its specific heat **[23, 26]**. Specific heat of the nanoparticle was $880\,J/kgK$ in the calculations and taken from Refs. **[16, 27].** Yu and Choi used the Eq. below to determine the thermal conductivity of the nanofluids **[28]**.

Thermal conductivity of nanofluids,

$$k_{nf} = \left[\frac{k_{np} + 2k_s + 2\left(k_{np} - k_s\right)(1+\beta_l)^3\emptyset_{np}}{k_{np} + 2k_s - \left(k_{np} - k_s\right)(1+\beta_l)^3\emptyset_{np}}\right]k_s \quad (5)$$

In Eq. (5), β_l refers to the nano-layer thickness and the nanoparticle radius is considered between 19% and 22% in general **[29]**. In the calculation of the thermal conductivity, $\beta_l = 0.2$ was considered and the thermal conductivity of the nanoparticle was taken as $k_{np} = 35\,W/m^2K$ from Ref. **[27]**. For the temperature-dependent thermophysical characteristics of the distilled water, temperature-dependent

Eq.s were obtained from Ref. **[30]** by using the characteristics of the water between $0-100$ ℃ as follows:

For density,

$$\rho_s = 1001.07 - 0.0885789\text{x}T - 0.00346617\text{x}T^2 \quad (R^2 = \%99.94) \tag{6}$$

For dynamic viscosity,

$$\mu_s = 0.00175015 - 0.0000517503\text{x}T + 8.65854\text{x}10^{-7}\text{x}T^2 - 7.53662\text{x}10^{-9}\text{x}T^3$$
$$+2.58918\text{x}10^{-11}\text{x}T^4 \quad (R^2 = \%99.99) \tag{7}$$

For specific heat,

$$c_{p,s} = 4217.25 - 3.01528\text{x}T + 0.0780849\text{x}T^2 - 8.10854\text{x}10^{-4}\text{x}T^3$$
$$+3.32379\text{x}10^{-6}\text{x}T^4 \quad (R^2 = \%99.61) \tag{8}$$

For thermal conductivity,

$$k_s = 0.559434 + 0.00215742\text{x}T - 0.00000965824\text{x}T^2 \ (R^2 = \%99.98) \tag{9}$$

Here, the subscripts nf, np and s express nanofluid, nanoparticle and distilled water, respectively.

2.3. Experimental setup and procedure

The experimental setup of the corrugated surfaced plate, which was established to investigate the heat transfer and pressure drop characteristics under different flow conditions, has been given in Fig. 1. Corrugated surfaced plate stands for a gasket plate heat exchanger and is supplied from Alfa Laval (T2

1. Power panel, **2.** Hot water tank, **3.** Nanofluid tank, **4.** Pumps, **5.** Test section, **6.** Pressure difference, **7.**Thermocouples, **8.** Hot water tank temperature indicator and frequency control panel of pumps, **9.** Data logger, **10.** Hot water flow meter, **11.** Cold nanofluid flow meter and indicator, **12.** Power panel, **13.** Nanofluid temperature control and indicator, **14.** Computer, **15.** Chiller.

(a)

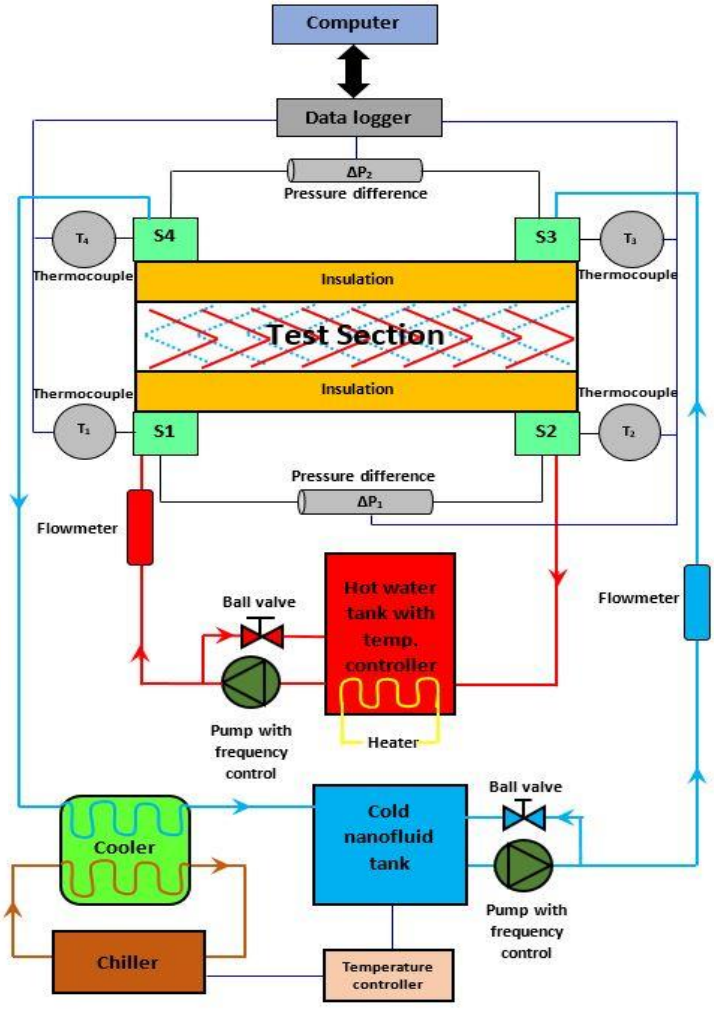

(b)

Fig.1. (a) Photo of test rig. (b) Schematic of the experimental setup.

model) firm. Geometrical details of the corrugated surfaced plate have been given in Tab. 1, and the basic dimensions have been given in Fig. 2.

There are two loops in the experimental set up as heat remover (hot fluid) and heat absorber (cold fluid) fluids, as in Fig. 1. Hot fluid (hot water) is provided from an insulated tank with the capacity of 90 L and immersion heater resistance at 2 kW. Moreover, this tank sets the desired temperature value of the hot fluid at the inlet to the plate heat exchanger with a temperature controlled device. A float rotameter was used to measure the flow rate of the hot fluid. The cold fluid (nanofluids) was stored in a 16 L tank mixed mechanically for the homogenous dispersion of the nanoparticles during the experiments. A temperature controlled cooler has been used to ensure the constant temperature of the nanofluids at the inlet to the plate heat exchanger, and its flow rate was measured by an indicator connected to the turbine-type flow meter. A differential diaphragm pressure gauge was placed between the inlet and outlet ports to measure the differential pressures of the hot water and nanofluids. A highly sensitive Pt-100 thermocouple pair was used to measure the temperatures of each fluid at the inlet and outlet of the plate heat exchanger. Circulation of the hot water and nanofluids was ensured with centrifugal pumps which are 120^{o}C heat resisting. Moreover, test section and pipes were insulated to minimize the heat loss.

Table 1. Geometrical properties of the gasket plate heat exchanger used in the study

Plate length (mm)	350
Plate width (mm)	102
Plate width inside gasket, L_w (mm)	70
Vertical distance between centers of ports, L_v (mm)	298
Horizontal distance between centers of ports, L_h (mm)	50
Port diameter D_{pt}, (mm)	20
Number of plates	3
Heat transfer area, A(m^2)	0.02
Gap between two consecutive plate, (mm)	2.4
Plate thickness, t(mm)	0.5
Plate pitch, p (mm)	3.05
Corrugation pitch, P_c(mm)	11.57
Mean channel spacing, b(mm)	2.5
Chevron angle, β	30^{o}

Experiments were conducted at the room temperature and under steady-state conditions. Also temperature and differential pressure values measured during the experiments were recorded on the computer. During the experiments, the flow rate of the hot water was 90 kg/h and the plate heat exchanger inlet temperature was constant at 40^{o}C. While the flow rate of the nanofluids varied between 90 and 300 kg/h, the inlet temperature of the cold fluid was 17.5^{o}C.

2.4. Data Analysis

Heat transfer and pressure drop characteristics of the plate heat exchanger were calculated by means of the experimental data. When the hydraulic diameter of the plate heat exchanger and the mass flow rate of the channel are based on, Reynolds numbers of the hot water and nanofluids are as follows.

$$Re_{hw} = G_{hw} D_h / \mu_{hw} \tag{10}$$

$$Re_{nf} = G_{nf} D_h / \mu_{nf} \tag{11}$$

Here, D_h refers to the hydraulic diameter, G_{nf} and G_{hw} stand for the mass velocities of the channel for the cold and hot fluids.

$$G_{hw} = \dot{m}_{hw}/N_{cp}bL_w \quad (12)$$

$$G_{nf} = \dot{m}_{nf}/N_{cp}bL_w \quad (13)$$

Heat removed by the hot water and absorbed by the nanofluids has been calculated with the Eq. (14)-(15) by using the measured temperature and flow rate values and calculating specific heat values.

$$Q_{hw} = \dot{m}_{hw}c_{p,hw}\left(T_{hw,i} - T_{hw,o}\right) \quad (14)$$

$$Q_{nf} = \dot{m}_{nf}c_{p,nf}\left(T_{nf,i} - T_{nf,o}\right) \quad (15)$$

Theoretically, these two values are equal, but the difference between these values is maximum 5%. Therefore, the average heat transfer values were used in the calculations due to the heat loss of both fluids.

$$Q_{ave} = (Q_{hw} + Q_{nf})/2 \quad (16)$$

Thermodynamic characteristics of both fluids were calculated by using the average temperature values at the inlet and outlet of the plate heat exchanger.

$$T_{ave,hw} = (T_{hw,i} + T_{hw,o})/2 \quad (17)$$

$$T_{ave,nf} = (T_{nf,i} + T_{nf,o})/2 \quad (18)$$

In many studies carried out in the literature on the plate heat exchanger, the Nusselt number is regarded as a function of the Re number, the Prandtl number and as the ratio of the dynamic viscosities at the average fluid temperature and the wall temperature. The general correlation expression for the turbulent flow is **[31, 32]**:

$$Nu = CRe^n Pr^m \left(\mu_b/\mu_w\right)^d \quad (19)$$

Heat transfer coefficient of the hot fluid in the plate heat exchanger h_{hw} was calculated, (assumption,$\mu_b \cong \mu_w$)

$$Nu_{hw} = CRe_{hw}^n Pr_{hw}^m \quad (20)$$

Here, *C*=0.348, *n*=0.663 and *m*=0.33; they change according to the flow characteristics and the chevron angle. General expressions; for Eq. (21)-(22), the Nusselt and Prandtl numbers are as follows:

$$Nu = hD_h/k \quad (21)$$

$$Pr = \mu c_p/k \quad (22)$$

When the experimental data are based on, the overall heat transfer coefficient is as follows;

$$U = Q_{ave}/A\Delta T_{lm} \quad (23)$$

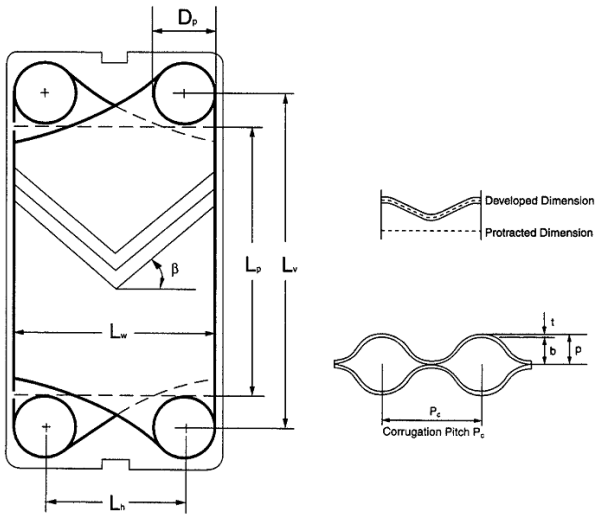

Fig. 2. Basic dimensions of the gasket plate heat exchanger.

Here,

$$\Delta T_{lm} = \frac{\left(T_{hw,i} - T_{nf,o}\right) - \left(T_{hw,o} - T_{nf,i}\right)}{In\left[\left(T_{hw,i} - T_{nf,o}\right)/\left(T_{hw,o} - T_{nf,i}\right)\right]} \tag{24}$$

The heat transfer coefficient of the nanofluids has been found from the relationship below.

$$\frac{1}{U} = \frac{1}{h_{hw}} + \frac{t_w}{k_w} + \frac{1}{h_{nf}} \tag{25}$$

The pressure drop of the nanofluids and hot water was calculated depending on the experimental data. The friction factor is calculated from the relationship below. The pressure drop at the ports of the heat exchanger (26):

$$\Delta P_{pt} = 1.4 N_p (G_{pt}/2\rho) \tag{26}$$

$$G_{pt} = (\dot{m}/(\pi D_{pt}^2/4)) \tag{27}$$

Here D_{pt} refers to the inlet diameter and, N_p stands for the number of passes, while G_{pt} symbolizes the mass flow rate of the inlet port.

$$\Delta P = \Delta P_{experimental} - \Delta P_{pt} \tag{28}$$

$$f = \Delta P/[(L_{eff}/D_h)(2G^2/\rho)] \tag{29}$$

Here, f is the friction factor, L_{eff} is the vertical distance at the inlet and outlet of the heat exchanger, and the enlargement factor of the corrugated surface φ is taken into account, since $L_{eff} = L_v$. Rheological and thermophysical characteristics of the nanofluids were calculated using the average temperature. Then, the Nu number and heat transfer coefficient were obtained for different volume concentrations.

2.5. Experimental Uncertainties

In the plate heat exchanger, temperature, pressure drop and flow rate values were measured with the appropriate equipment during the experiments. While measuring these values, uncertainties appeared because of the friction and electronic releases. These errors were calculated using the Eq. expressed by Kline and McClintock **[33]**.

$$W_R = [\left(\frac{\partial R}{\partial x_1} w_1\right)^2 + \left(\frac{\partial R}{\partial x_2} w_2\right)^2 + \ldots\ldots\ldots\ldots + \left(\frac{\partial R}{\partial x_n} w_n\right)^2]^{1/2} \quad (30)$$

For an R function given here, $x_1, x_2, \ldots x_n$ give the independent variables, $w_1, w_2, \ldots w_n$ gives the ratio of the independent variable and w_R gives the total uncertainty. Relative errors of uncertainties during the measurements of the measuring equipment are as follows; ± 0.4%, ± 0.4%, ± 5%, ± 3%, ± 1%, ± 0.5% for hot fluid inlet and outlet temperature, nanofluids inlet and outlet temperature, turbine flow meter, rotameter, table values, differential pressure, plate dimensions, respectively. Uncertainty values that emerged during the experiments were calculated and illustrated in Tab. 2. It was observed that all the experimental data, which were obtained with the repeated experiments, existed within the limits of uncertainty.

3. Results and discussions

In the experimental setup in Fig. 1, testing experiments were performed for heat transfer from hot water to cold distilled water in order to evaluate the accuracy and reliability of the measurements before calculating the heat transfer coefficient of the nanofluids. After all the measurements, the overall heat transfer coefficient was estimated from Eq. (23) and the heat transfer coefficient for the hot fluid was estimated from Eq. (20).The heat transfer coefficient for the cold fluid was obtained from Eq. (25). As shown in Fig. 3, it can be observed that the experimental overall heat transfer coefficient calculated for distilled water from Eq. (23) and the overall heat transfer coefficient calculated theoretically are in concordance, and the error is 3% on average.

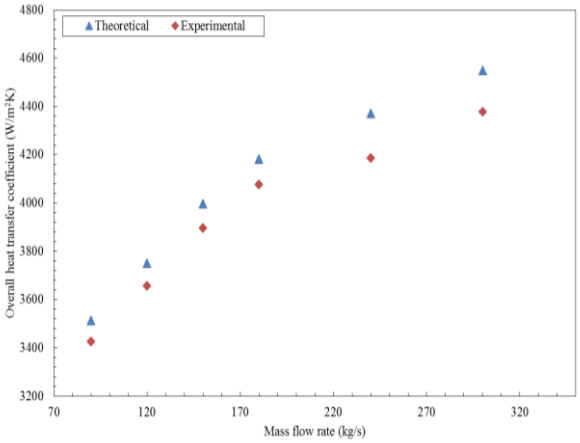

Fig. 3. Comparison of the theoretical and experimental overall heat transfer coefficients

In this study, the Re number has been found to range between 600 and 1900 at the 0.25%, 0.5%, 0.75% and 1% volume concentration of the Al_2O_3/water nanofluids, and the overall heat transfer coefficients, heat transfer coefficients, Nu numbers and pressure drops, which belonged to the nanofluids, were obtained for 90 kg/h flow rate of the hot water.

Table 2. Results of total uncertainty

Hot fluid side Reynold number	2.42%
Nanofluids side Reynold number	3.07%
Heat transfer	7.39%
Overall heat transfer coefficient	6.52%
Friction factor	8.74%

The constant inlet temperatures and the mass flow rate that increased at the fix volumetric concentration caused the high heat transfer coefficient. An efficient mechanism for this increase, the

particles added to the fluid enhanced the heat transfer. Another efficient mechanism for the enhancement of the heat transfer is the thermal conductivity that increases as a result of the collision between the water molecules on the wall surface of the plate heat exchanger and the nanoparticles. Eq. (5) used in the calculation of the thermal conductivity of the nanofluid is also considered in the intermediate surface between the fluid and the particles since heat transfer between the particles and the fluid occurs in the intermediate surfaces of the particle. Breakdown occurs in the thermal boundary layer and its thickness decreases depending on the movement of the particles in the areas close to the surface, the continuous change in the direction and velocity of the particles within the channel, and the decrease in the effect of viscosity in the areas close to the surface in the plate heat exchanger.While these interactions enhanced the heat transfer, they also increased the friction between the plate heat exchanger surface and the nanofluids. The highest increase in the overall heat transfer occurs at 1% volume concentration against the flow rates of the nanofluid and the fix hot fluid. This increase is 29.42%, 24.34%, 18.02%, 15.37%, 11.74% and 9.43% for the 90, 120, 150, 180, 240 and 300 kg/h nanofluids flow rate, respectively. Furthermore, the difference between the inlet and outlet temperatures of the plate heat exchanger decreases and the amount of transferred heat increases while the flow rate and volume concentration of the nanofluids increase. Specific heat of the nanofluids

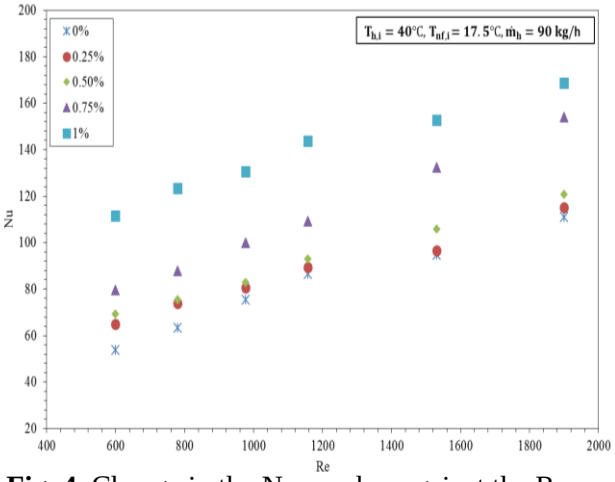

Fig. 4. Change in the Nu number against the Re number of the water and the Al_2O_3 nanofluids

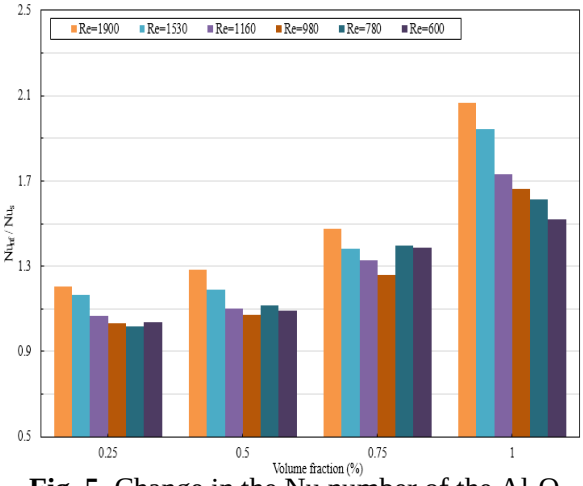

Fig. 5. Change in the Nu number of the Al_2O_3 nanofluids compared to water

decreases with the addition of the particles into the water. This change is inversely proportional to the volume concentration of the particles.

The decrease in the specific heat caused rapid temperature changes in the plate heat exchanger. Results obtained for the overall heat transfer coefficient indicate that the presence of nanoparticles in water increased the overall heat transfer coefficient. In Fig. 4, the change in the Nu number against the Re number of the nanofluids is observed for the prepared concentrations. As seen in Fig. 4, the Nu number increases with the increase in the nanoparticle concentration in case of the constant Re number, and the Nu number of the nanofluids is higher than that of the water. As the mass flow rate of the nanofluids increased and the collision interactions of the nanoparticles increased on the surfaces of the plate heat exchanger, the amount of the heat transferred to the nanofluids increased accordingly. Fig. 5 shows the ratio of the calculated Nu number of the nanofluids to the Nu number of the water at different concentrations and Re numbers. This ratio increases with an increase in the Re number and volume concentration. For example, the increase rate in the Nu number of the nanofluids ranges between 1.52 and 2.07 while the Re number varies between 600 and 1900 at 1% volume concentration. Another result obtained from this study is the change in the density and viscosity of the nanofluids due to the particles added to the water. As the nanoparticle concentration increases, the viscosity and density of the fluid increase, too and this leads to the pressure drop.

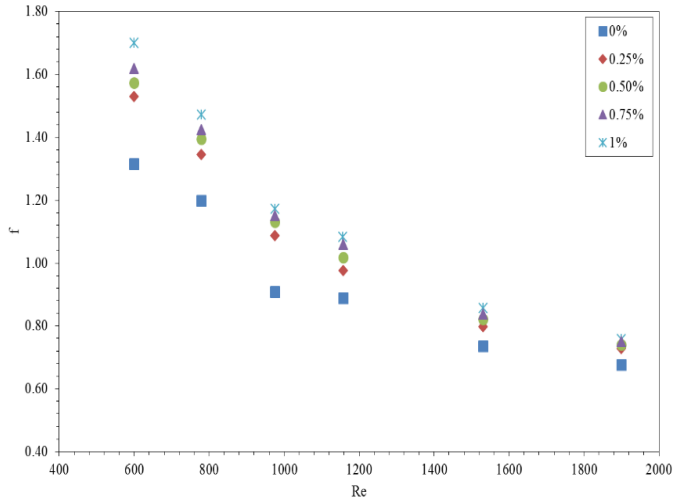

Fig. 6. Change in the friction factor of the water and the Al_2O_3 nanofluids against the Re number

The pressure drop of the nanofluids was calculated with Eq. (29), and the change in the friction factor was obtained in Fig. 6 against the Re number. Pressure drop increased with the increasing volume concentration in the constant Re number. Minimum pressure drops were obtained for water, and pressure drop increases in high Re numbers. Such a pressure drop is also valid for the prepared nanofluids. The pressure drop of the nanofluids prepared at maximum Re numbers presents an increase between 6.4% and 8.4% compared to water. Viscosity has a low effect on the pressure drop and friction factor, and the density has a higher effect as it can be observed in Eq. (29). Thus, it is clearly understood that the convection heat transfer coefficient increased because of the change in the characteristics of the working fluid that enables the heat transfer by using the nanofluids in the plate heat exchanger. At 90 kg/h hot water flow rate, an increase occurs in the heat transfer of the Al_2O_3/water nanofluids together with the increasing volume concentration and the flow rate. The usage of the nanofluids in the plate heat exchangers enhanced the heat transfer and the performance of the systems and hence presented advantages for increasing the energy efficiency. Besides, pressure drops increased while the performance of the plate heat exchanger was increased by using nanofluids. Nanofluids can be reasonable solutions for enhancing the heat transfer; however, a totally opposite situation emerges in terms of the pressure drop depending on the selected volume concentration. This potential of the nanofluids draws attention in the heat transfer.

4. Conclusion

In this study, the Nu number and pressure drops in the plate heat exchanger were experimentally investigated for the Al_2O_3/water nanofluids. Experiments were conducted at 4 different volume concentrations (0.25%, 0.5%, 0.75%, 1%), fix hot fluid flow rate and temperature. It was concluded that the Nu number increased depending on the increasing Re number of the nanofluids and the volume concentration. In enhancing the heat transfer, dispersion of the nanoparticles within the fluid, irregular movement of the particles and the transport of the particles are the factors leading an increase in the heat transfer besides an increase in the thermal conductivity of the nanofluids. Fluctuation of the particles and their effects with the fluid especially led to a change in the flow structure in high Re numbers. When the pressure drop of the nanofluids was compared with the pressure drop of the water in the Re number and at the selected volume concentration, an increase varying between 6% and 20% occurred. For this reason, the selected concentration and the flow rate can be appropriate for practical

applications. The experimental results indicate that the increase was achieved between 7.72%, 12.07%, 26.91%, and 42.4%, respectively, on average in the Nu number for the nanofluids at the selected 0.25%, 0.5%, 0.75%, 1% volume concentrations and Reynolds number varying between 600 and 1900. The pressure drop of the nanofluids is approximately the same as those of water maximum Re number. For the studies operating ranges, average 22% improvement of heat transfer coefficient has been found by using nanofluids.

Acknowledgements

This work was supported by Research Fund of the Sakarya University. Project Number: 2013-01-06-033.

Nomenclature

A	heat transfer area, m^2
b	mean channel space , m
c_p	specific heat at constant pressure, J $kg^{-1}K^{-1}$
D_h	hydraulic diameter, m
D	diameter, m
f	friction factor
G	mass velocity, kg $m^{-2}s^{-1}$
h	convective heat transfer coefficient, $Wm^{-2}K$
k	thermal conductivity, Wm^{-1} K^{-1}
L_{eff}	effective flow length between inlet and outlet port, m
L_w	effective channel width, m
$\dot{m}$	mass flow rate, kg s^{-1}
m	mass, kg
N_{cp}	number of channels per pass
Nu	Nusselt number
Q	heat transfer rate, W
Pr	Prandtl number
Re	Reynolds number
T	temperature, ^oC
t	thickness of plate, m
U	overall heat transfer coefficient, W m^{-2} K^{-1}
w	total uncertainty in the measurement

Greek symbols

β	chevron angle, degree
β_l	nano-layer thickness
ΔT_{lm}	logarithmic mean temperature difference, K
ΔP	pressure drop, Pa
μ	viscosity, Ns m^{-2}
ρ	density, kg m^{-3}
φ	enlargement factor
∅	volumetric concentration

Subscripts

hw	hot water
i	inlet condition
nf	nanofluid
np	nano particle
o	outlet condition
p	passes
pt	port
s	water
w	wall

References

[1] Maxwell, J.C., Treatise on Electricity and Magnetism, Second ed. Oxford Univ. Press, Cambridge, UK, 1904.

[2] Choi, S.U.S., Developments and Application of Non-Newtonian Flows, ASME FED-V.231/MD-V.66, New York, 1995. 99–105.

[3] Zhai, Y.L., Xia, G.D., Liu, X.F., Li, Y.F., Heat transfer enhancement of Al2O3-H2O nanofluids flowing through micro heat sink with complex structure, International Communications in Heat and Mass Transfer 66 (2015) 158 –166.

[4] Tuckerman, D.B., Pease, R.F.W., High-performance heat sinking for VLSI, IEEE Electr. Dev. Lett. EDL-2 (1981) 126–129.

[5] Daungthongsuk, W., Wongwises, S., A critical review of convective heat transfer of nanofluids, Renew. Sust. Energy Rev. 11 (2007) 797–817.

[6] Nandigana, V., Selvaraju, N., Mahadevan, K., Convective heat transfer coefficient of nanofluids. Lambert Academic Publishing, Germany, 2012.

[7] Heris, S. Z., Etemad, S.Gh., Esfahany, M. N., Experimental investigation of oxide nanofluids laminar flow convective heat transfer, International Communications in Heat and Mass Transfer 33 (2006) 529–535.

[8] Anoop, K.B., Sundararajan, T., Das, S. K., Effect of particle size on the convective heat transfer in nanofluid in the developing region, International Journal of Heat and Mass Transfer 52 (2009) 2189–2195.

[9] Xu, L., Xu, J., Nanofluid stabilizes and enhances convective boiling heat transfer in a single microchannel, International Journal of Heat and Mass Transfer 55 (2012) 5673–5686.

[10] Edalati, Z., Heris, S. Z., Noie, S.H., The Study of Laminar Convective Heat Transfer of CuO/WaterNanofluid Through an Equilateral Triangular Duct at Constant Wall Heat Flux, Heat Transfer- Asian Research, 41 (5), 2012.

[11] Hojjat, M., Etemad, S. Gh., Bagheri, R., Thibault, J., Laminar convective heat transfer of non-Newtonian nanofluids with constant wall temperature, Heat Mass Transfer (2011) 47:203–209.

[12] Sommers, A. D., Yerkes, K. L., Experimental investigation into the convective heat transfer and system-level effects of Al_2O_3 -propanol nanofluid, J. Nanopart Res (2010) 12:1003–1014.

[13] Tiwari, A. K., Ghosh, P., Sarkar, J., Heat transfer and pressure drop characteristics of CeO_2/water nanofluid in plate heat exchanger, Applied Thermal Engineering 57 (2013) 24-32.

[14] Huang, D., Wu, Z., Sunden, B., Pressure drop and convective heat transfer of Al_2O_3/water and MWCNT/water nanofluids in a chevron plate heat exchanger, International Journal of Heat and Mass Transfer, 89 (2015) 620–626.

[15] Heris, S. Z., Esfahany, M. N., Etemad, S.Gh., Experimental investigation of convective heat transfer of Al_2O_3/water nanofluid in circular tube, International Journal of Heat and Fluid Flow 28 (2007) 203–210.

[16] Mangrulkar, C.K., Kriplani, V. M., Dhoble, A. S., Experimental investigation of convective heat transfer enhancement using alumina/water and copper oxide/water nanofluids, Thermal science, 2015.

[17] Haddad, Z., Abid, C., Oztop, H.F., Mataoui, A., A review on how the researchers prepare their nanofluids, International Journal of Thermal Sciences 76 (2014) 168-189.

[18] Ali, H. M., Azhar, M. D., Saleem, M., Saeed, Q. S., SAIEED, A., Heat transfer enhancement of car radiator using aqua based magnesium oxide nanofluids, Thermal science, 2015.

[19] Haddad, Z., Eiyad, A.N., Oztop, H.F., Mataoui, A., Natural convection in nanofluids: Are the thermophoresis and Brownian motion effects significant in nanofluid heat transfer enhancement, International Journal of Thermal Sciences 57 (2012) 152-162

[20] Pak, B.C., Cho. Y.I., Hydrodynamic and heat transfer study of dispersed flids with submicron metallic oxide particles, Experimental Heat Transfer 11, 1999, 151–170.

[21] Drew, D.A., Passman, S.L., Theory of Multi component Fluids. Springer, Berlin, 1999

[22] Ho, C.J., Liu, W.K., Chang, Y.S., Lin, C.C., Natural convection heat transfer of alumina-water nanoflid in vertical square enclosures: An experimental study, International Journal of Thermal Sciences 49, 2010, 1345–1353.

[23] Minkowycz, W. J., Sparrow, E. M., Abraham, J. P., Nanoparticle Heat transfer and fluid flow, CRC Press, Volume IV, Taylor & Francis Group, New York, 2013.

[24] Einstein, A., Investigations on the Theory of the Brownian Movement, Dover Publications, New York, 1956.

[25] Abdellahoum C., Mataoui A., Oztop H.F., Comparison of viscosity variation formulations for turbulent flow of Al2O3–water nanofluid over a heated cavity in a duct, Advanced Powder Technology 26 (2015) 1210–1218.

[26] Xuana, Y., Roetzel, W., Conceptions for heat transfer correlation of nanofluids, International Journal of Heat and Mass Transfer 43 (2000) 3701-3707.

[27] Sundar, L. S., Farooky, Md. H., Sarada, S. N., Singh, M.K., Experimental thermal conductivity of ethylene glycol and water mixture based low volume concentration of Al2O3 and CuO nanofluids, International Communications in Heat and Mass Transfer 41 (2013) 41–46.

[28] Yu W., Choi, S.U.S., The role of international layers in the enhanced thermal conductivity of nanofluids: A renovated Maxwell model, Int. J. Heat and Fluid Flow 28 (2007) 203–210.

[29] Tillman, P., Hill, J. M., Determination of nanolayer thickness for a nanofluid, International Communications in Heat and Mass Transfer 34 (2007) 399 – 407.

[30] Cengel, Y. A., Introduction to Thermodynamics and Heat Transfer, McGraw-Hill, Second Edition, 2007.

[31] Kakac, S., Liu, H., Heat Exchangers: Selection, Rating and Thermal Design, Third edition, CRC Press, USA, 2012.

[32] Shah, R. K., Sekulic, D. P., Fundamentals of heat exchanger design, John Wiley & Sons, Inc., USA, 2003.

[33] Holman, J.P., Experimental Methods for Engineers, Eighth edition, McGraw-Hill, New York, 2011.